Neuron, Vol. 30, 437–450, May, 2001, Copyright ©2001 by Cell Press

# N-Cadherin Regulates Target Specificity in the *Drosophila* Visual System

**Chi-Hon Lee,[2] Tory Herman,[2] Thomas R. Clandinin,[2] Roger Lee, and S. Lawrence Zipursky[1]**
Department of Biological Chemistry
Howard Hughes Medical Institute
University of California, Los Angeles
School of Medicine
5-748 MRL
675 Charles Young Drive South
Los Angeles, California 90095

## Summary

**Using visual behavioral screens in *Drosophila*, we identified multiple alleles of *N-cadherin*. Removal of N-cadherin selectively from photoreceptor neurons (R cells) causes deficits in specific visual behaviors that correlate with disruptions in R cell connectivity. These defects include disruptions in the pattern of neuronal connections made by all three classes of R cells (R1–R6, R7, and R8). N-cadherin is expressed in both R cell axons and their targets. By inducing mitotic recombination in a subclass of eye progenitors, we generated mutant R7 axons surrounded by largely wild-type R cell axons and a wild-type target. R7 axons lacking N-cadherin mistarget to the R8 recipient layer. We consider the implications of these findings in the context of the proposed role for cadherins in target specificity.**

## Introduction

Neurons form exquisitely precise patterns of synaptic connections. How this is achieved during development remains a central issue in neurobiology. Remarkable progress has been made in identifying signals and receptors that play crucial roles in guiding axons to their target regions (Tessier-Lavigne and Goodman, 1996) and in dissecting the molecular basis for topographic map formation (Flanagan and Vanderhaeghen, 1998). In contrast, we know little about how neurons select specific cells or layers within the target region with which to make synaptic connections.

Cadherins form a large family of transmembrane proteins (Yagi and Takeichi, 2000) that can mediate both strong homophilic (Miyatani et al., 1989), as well as weak heterophilic interactions (Shan et al., 2000). Functional studies in vertebrates and genetic studies in *Drosophila* have demonstrated that cadherins play broad roles in nervous system development (Iwai et al., 1997; Riehl et al., 1996; Detrick et al., 1990; Inoue and Sanes, 1997). Recently, cadherins have been proposed to regulate target specificity and synapse formation (Fannon and Colman, 1996). Many cadherins are expressed in a region-specific fashion in the vertebrate brain (Yamagata et al., 1995; Miskevich et al., 2000), their distributions are dynamically regulated during development (Fannon and Colman, 1996; Suzuki et al., 1997; Wohrn et al., 1999), and they have been localized to synaptic regions at both the pre- and postsynaptic membranes (Uchida et al., 1996; Kohmura et al., 1998; Fannon and Colman, 1996). It has, therefore, been proposed that different neurons express distinct cadherins whose selective adhesive properties underlie the selection of synaptic partners. This model has not yet been critically assessed through genetic analysis.

In behavioral screens for mutations affecting photoreceptor (R cell) targeting, we identified multiple alleles of *Drosophila N-cadherin*. The *Drosophila* compound eye contains an array of some 800 ommatidia, each containing eight R cells (R1–R8 cells). The R1–R6 cells are sensitive to green light (Harris et al., 1976) and connect to targets in the first optic ganglion, the lamina. R7 and R8 cells are responsive to ultraviolet and blue light (Harris et al., 1976), respectively, and form synapses with processes in two distinct layers in the second optic ganglion, the medulla (Meinertzhagen and Hanson, 1993). In addition to ganglion and cell-type specificity, R cells elaborate a topographic map in both the lamina and the medulla. Here we show that removal of N-cadherin from all R cells causes severe and complex defects in the pattern of R cell connections. Removal of N-cadherin from a small number of R7 neurons only, however, causes a precise defect in target specificity. Mutant R7 neurons do not extend to the R7 recipient layer, but instead terminate incorrectly in the R8 recipient layer. This selective defect in R7 target specificity leads to a striking deficit in visual behavior. We consider the significance of these findings in the context of the proposed role for cadherins as regulators of synaptic target specificity in vertebrates.

## Results

### N-Cadherin Is Required in R Cells to Mediate a Subset of Visual Behaviors

We have undertaken a behavioral approach to identifying loci that function specifically within R cells to control R cell connectivity. We created mosaic animals whose retinas alone were homozygous for randomly mutagenized chromosomes, while their remaining tissues were wild-type (Newsome et al., 2000; Stowers and Schwarz, 1999). We then tested their ability to perform two retina-dependent behavioral tests: an optomotor assay to assess the function of R1–R6 (Heisenberg and Buchner, 1977) and a UV/Vis light choice assay to assess the function of R7 (Gerresheim, 1981; Reinke and Zipursky, 1988). Both of these behavioral assays were sensitized such that the response of wild-type flies was close to threshold. We anticipated that our approach would identify a large number of loci required for many different aspects of R cell function and that a subset of these loci would regulate R cell connectivity. A detailed description of these screens will be published elsewhere.

[1]Correspondence: zipursky@hhmi.ucla.edu
[2]These authors contributed equally to this work.

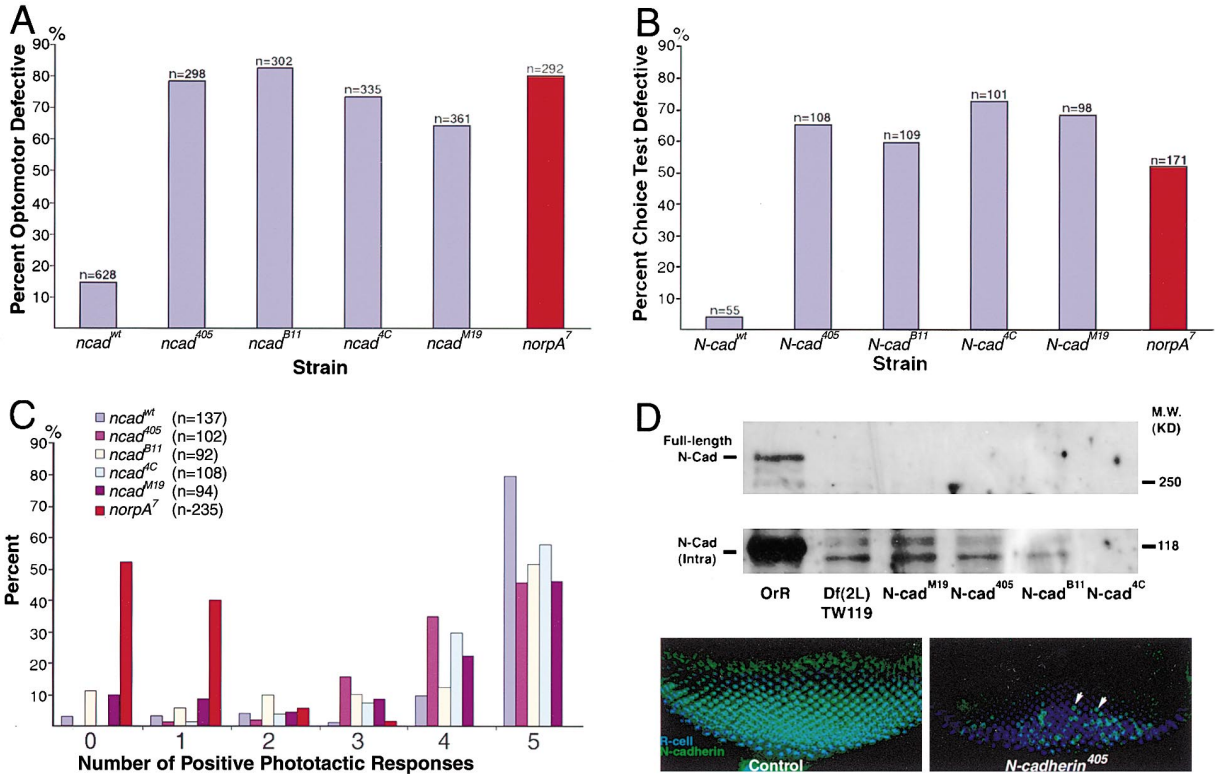


Figure 1. N-Cadherin Activity Is Required in R Cells for Visual Behaviors

The visual responses of somatic mosaic animals whose retinas, including all R cells, were homozygous for a series of *N-cadherin* alleles and whose remaining tissues were wild-type were assayed using three different behavioral tests. In each assay, eye-specific mosaic, wild-type FRT40A flies were used as controls. As a negative control *norpA*, a phototransduction mutant, was used (red bars).

(A) The optomotor response. Each genotype was tested six times and the percentage of the flies that failed to move an arbitrary distance (27 cm) into a collection tube is plotted on the y axis (see text). The genotype of retina is indicated on the x axis. In this assay, the ability of *N-cadherin* mutant flies to detect motion is approximately 5-fold worse than wild-type.

(B) The UV/Vis choice test. Each genotype was tested three times and the percentage that chose visible light is plotted on the y axis (see text). The genotype of retina is indicated on the x axis. In this assay, the response of *N-cadherin* mutant flies is approximately 8-fold worse than wild-type.

(C) The counter-current fast phototaxis assay. In this assay, groups of approximately 35 flies are placed at one end of tube and a bright visible light is shone on the other end. Flies that moved toward the light source were scored as positive and were separated from those that failed to respond. Each group was tested five times. The x axis plots the number of times, out of five trials, that flies responded positively to the light source. The y axis plots the percentage of the group that fell into each response category. Three groups for each *N-cadherin* allele were tested for this behavior. In this assay, *N-cadherin* mosaic flies responded well, although their response was reduced compared to wild-type. Independent experiments demonstrated that blind flies fail to respond under these experimental conditions and remain in the 0–2 classes. In all of these assays, variation between trials was statistically insignificant and the results from all trials were pooled.

(D) N-cadherin protein was absent from *N-cadherin* mutant embryos (upper panels). The bands corresponding to full-length N-cadherin (approximately 300 kDa), and the processed C-terminal fragment (120 kDa) are indicated. Each allele was assessed as heterozyotes over a deficiency removing the entire locus. In the middle panel, the two bands seen in a complete deficiency for the locus represent cross-reactive bands. N-cadherin protein was also absent in homozygous mutant clones in the eye imaginal disc generated by mitotic recombination using ey-FLP. Scattered N-cadherin-expressing cells are likely heterozygous or wild-type cells also generated by mitotic recombination. N-cadherin and HRP (a neuron specific marker) immunoreactivity are green and blue, respectively.

Using these screening strategies, we isolated three mutations in *N-cadherin* that disrupted both R1–R6- and R7-specific behaviors (Figure 1). In particular, we identified one allele of *N-cadherin*, designated *N-cadherin*$^{405}$, using the optomotor assay and two alleles, designated *N-cadherin*$^{B11}$ and *N-cadherin*$^{4C}$, using the UV/ Vis choice test. All phenotypic analyses of these mutations, unless otherwise noted, were conducted in mosaic animals in which only eye tissue was homozygous mutant.

All three of our *N-cadherin* alleles, as well as a previously isolated strong loss-of-function mutation of *N-cadherin*, *N-cadherin*$^{M19}$, caused strong defects in the R1–R6-specific optomotor response in eye-specific mosaics (Figure 1A). In this assay, wild-type flies placed at one end of a long, clear tube assess the direction of motion of a bar of visible light and move in the direction opposite to that of the bar's motion (S. Benzer, personal communication). Mutant flies that cannot detect the bar move randomly within the tube and thus can be separated from wild-type animals. This behavior is mediated by the visible light response of R1–R6 cells. Under these conditions, approximately 14% of wild-type flies failed to move a defined distance into a terminal collection tube within 1 min (Figure 1A). By contrast, in *N-cadherin*$^{405}$ and

*N-cadherin*$^{4C}$, approximately 78% and 73%, respectively, failed to move the same distance. *N-cadherin*$^{M19}$ and *N-cadherin*$^{B11}$ are also defective in this assay but have a mild defect in eye pigmentation that may also affect their optomoter response (T.R.C., unpublished data).

All four *N-cadherin* alleles also cause strong defects in the R7-specific UV/Vis choice test in eye-specific mosaic animals (Figure 1B). R7 neurons are the primary receptors of UV light: when wild-type flies are placed in a T maze with a source of green light at the end of one arm and a source of UV at the other, they phototax toward the UV source. Flies lacking R7 function instead phototax toward the visible source. In the case of each *N-cadherin* allele tested, a substantial portion of flies with mutant retinas chose visible light, suggesting that their R7 function is disrupted (Figure 1B).

*N-cadherin* mosaic flies are not completely blind. In another visual behavior, the fast phototaxis assay with countercurrent separation (Benzer, 1967), the ability of flies to phototax toward a strong source of visible, white light was quantified (Figure 1C). Under these test conditions, *N-cadherin* mosaic flies displayed strong phototactic responses that were only slightly weaker than those of control flies (Figure 1C). As a negative control, blind flies mutant for *norpA*, a gene essential for phototransduction, exhibited strong defects in the fast phototaxis and optomotor assays, and they showed no preference in the UV/Vis choice test.

That the three *N-cadherin* alleles isolated in the behavioral screen in this study are strong loss-of-function mutations is supported by genetic and biochemical data. The behavioral phenotypes associated with all three alleles were indistinguishable from the previously identified strong loss-of-function mutation, *N-cadherin*$^{M19}$. N-cadherin protein was not detected in Western blots of extracts prepared from homozygous mutant embryos probed with an antibody to the cytoplasmic domain (Figure 1D). N-cadherin immunoreactivity was greatly reduced or absent in mutant eye tissue as assessed using antibodies to either the N-terminal extracellular domain (data not shown) or the C-terminal cytoplasmic tail (Figure 1D).

## N-Cadherin Is Required for R Cell Axon Target Selection in the Lamina and Medulla

To determine whether the behavioral defects resulting from loss of N-cadherin function in the retina reflected defects in R cell connectivity, we first assessed the organization of R cell axon projections into the lamina and medulla (Figure 2). The organization of medulla structure was assessed in silver-stained sections (Heisenberg and Bohl, 1979; Gregory, 1980), while the R7 and R8 axons in the medulla were visualized using mAb24B10 (Fujita et al., 1982). As the precision of the R1–R6 connections in the lamina cannot be assessed with these techniques, these projections were visualized using DiI fills of single ommatidia (Clandinin and Zipursky, 2000).

### *N-Cadherin Activity in R Cells Controls Layer Formation in the Medulla*

While the overall organization of the adult optic lobe was unaffected in *N-cadherin* mosaic animals, the layered structure of the medulla was strongly disrupted (Figures 2A and 2B). In silver-stained preparations of wild-type animals, three darkly stained layers are prominent within the medulla (Figure 2A). These correspond to an outer layer of amacrine cell processes that separate the second medulla layer, designated M2, from the third layer, M3; a medial layer that defines M6 and an inner layer, designated the serpentine layer. In wild-type, R8 terminates within M3 while R7 terminates within M6 (Fischbach and Dittrich, 1989). In *N-cadherin* mosaic flies, we observed that all three of these darkly stained layers were severely disrupted, with the outer two layers completely lost, and with variable breaks in the serpentine layer (Figure 2B). These defects in layer formation are at least partially the result of R7 and R8 failing to reach their appropriate target layers. In wild-type adults, the regular array of R7 and R8 termini form two clearly separate layers that can be visualized with mAb24B10 (Figure 2C). By contrast, in *N-cadherin* mosaics, we observed that the R7 and R8 cells made highly irregular projections and frequently failed to penetrate into the appropriate medulla layer (Figure 2D). Using an R7-specific marker that labels R7 termini, we observed that the R7 array in the medulla of *N-cadherin* mosaics was severely disrupted and irregular with R7 termini found at various medulla layers (data not shown and see below). The result of these defects is that the separation of R7 and R8 termini into two distinct layers within the medulla is completely disrupted.

### *N-Cadherin Is Required in R Cells for R1–R6 Target Specificity*

In wild-type, the lamina contains a regular array of target neurons arranged in columns (Meinertzhagen and Hanson, 1993). R1–R6 axons from each ommatidial bundle migrate outward across the surface of the lamina and form synaptic contacts with a subset of cells within individual columns of target neurons, arranged in an invariant pattern. This association of R cell axons with lamina columns forms structures called cartridges.

To assess R cell target selection in the lamina, we injected fluorescent dye into single ommatidia and observed the pattern of projections formed using confocal microscopy (Figures 2E–2H). For technical reasons, this analysis cannot be done in adult animals, and hence the projections were assessed shortly after they formed during midpupal development. In wild-type animals, each R1–R6 cell from a single ommatidium makes a projection of characteristic length and polarity and forms connections in a different cartridge (Figures 2E and 2G). This projection pattern is initiated by defasciculation of R cell axons from the ommatidial bundle and requires specific interactions between R cell growth cones to form normally (Clandinin and Zipursky, 2000). In *N-cadherin* mutant animals, this pattern was severely disrupted in virtually all ommatidia (Figures 2F and 2H). While R1–R6 neurons targeted to the lamina (see below and Figures 3C and 3D), most R cell growth cones did not defasciculate or extend out from the ommatidial bundle to their targets (70/77 R cells scored in *N-cadherin*$^{M19}$; 22/22 R cells in *N-cadherin*$^{405}$). In rare cases, an R cell axon did extend outward (7/77 R cells in *N-cadherin*$^{M19}$; 0/22 cases in *N-cadherin*$^{405}$). The morphology of the R cell axons remaining within the ommatidial bundle was highly disrupted; each had a very thin growth cone with few filopodia (data not shown). These results suggest that N-cadherin activity is required for R

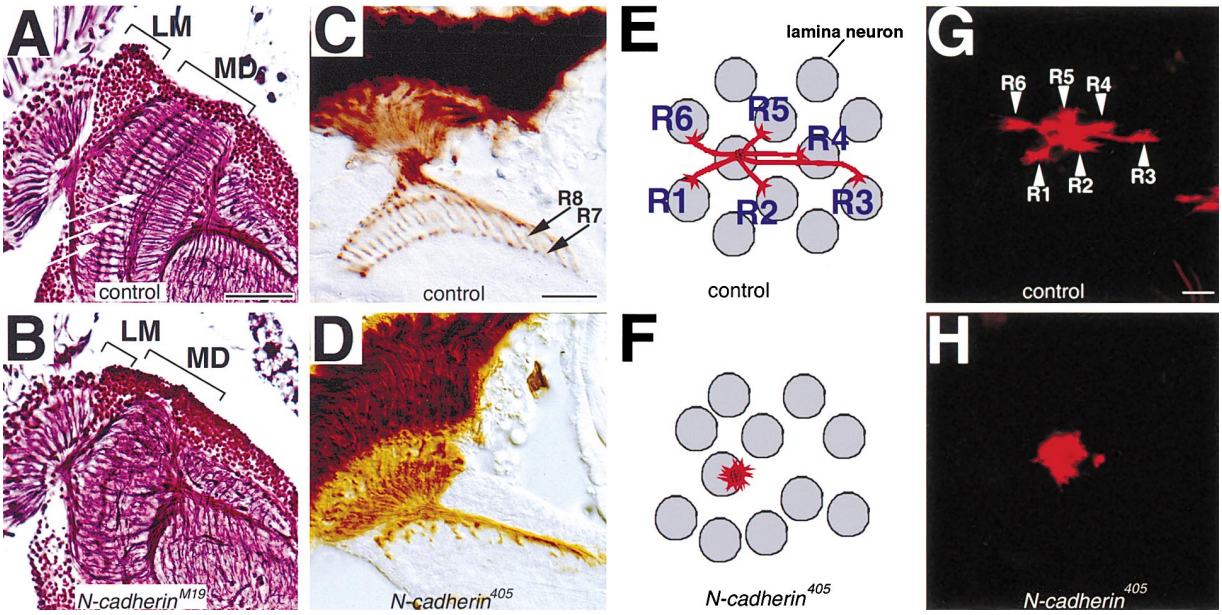


Figure 2. *N-Cadherin* Activity Is Required in R Cells for Visual System Connectivity

(A, C, E, and G) Isogenic control genotype, homozygous wild-type *N-cadherin*.

(B, D, F, and H) *N-cadherin* eye-specific mosaic animals.

(A and B) Silver-stained preparations of adult flies, viewed in horizontal sections. The retina is to the left of the frame. In (A), the white arrows point to the three prominently stained layers in the medulla of wild-type animals. The lower arrow denotes the boundary between M2 and M3; the middle arrow points to M6 and the upper arrow indicates the serpentine layer. In (B), the layered structure of the medulla is severely disrupted in *N-cadherin* mosaic animals. LM, lamina; MD, medulla.

(C and D) Cryostat horizontal sections of adult flies, stained with the R cell-specific mAb24B10. In (C), the R7 and R8 projections in wild-type form a regular array in the medulla (arrows). In (D), in *N-cadherin* mosaics, both R7 and R8 fail to form this array and often terminate at the outer edge of the medulla.

(E and F) Schematic illustration of the R1–R6 pattern of connections in the lamina. In wild-type (E), each R cell extends a projection (red) out of the ommatidial bundle that terminates within a regular array of lamina target neurons (gray circles). In *N-cadherin* mutant animals (F), all R cell growth cones fail to extend. In these animals, the relative positions of the lamina targets are also somewhat disordered. This disorder likely reflects earlier defects in the local topographic mapping of R1–R6 axons (see below; Figures 3E–3H).

(G and H) Dye-labeled projections of a single ommatidium during midpupal development. Fluorescent DiI was injected into single ommatidia and viewed using confocal microscopy in whole-mount animals. In wild-type, individual R cells make projections that occupy characteristic positions (indicated). *In N-cadherin* mosaic animals, R cell axons almost invariably fail to extend out of the ommatidial bundle. Individual growth cones corresponding to single R cells cannot be discerned; the smaller red dot is an R cell axon from a neighboring ommatidium.

Scale bars: 25 μm in (A) and (B); 20 μm in (C) and (D); 5 μm in (G) and (H).

cell growth cones to defasciculate from the ommatidial bundle. As a result, R1–R6 axons do not select the correct synaptic partners.

### *N-Cadherin Is Not Required for R Cell Differentiation*

To test whether the effects of *N-cadherin* mutations on R cell connectivity were caused by changes in R cell fate determination, we examined the development of *N-cadherin* mutant eye discs at the third larval stage using various cell-type specific markers. In particular, R cell differentiation (visualized using mAb24B10) in the *N-cadherin* mutant eye disc was normal, indicating that patterning of the eye disc proceeds as in wild-type (data not shown). Moreover, the expression patterns of all R cell-specific markers used (i.e., mδ-LacZ [for R4], Rotau-LacZ [for R2–R5], and PM181-Gal4 [for R7]) were indistinguishable from wild-type in the eye disc (data not shown), indicating that N-cadherin activity is not required for R cell fate determination. Finally, we examined toluidine blue stained sections of *N-cadherin* mosaic flies at the adult stage and observed, based on rhabdomere morphology and position, that the later stages of R cell differentiation occurred normally (data not shown).

### Loss of N-Cadherin Disrupts R Cell Projections as They Extend into the Developing Lamina and Medulla

To assess whether the targeting defects observed in the pupa and adult arise from very early defects in axon targeting to the lamina and medulla, we assessed the innervation pattern of R cell axons in the developing third larval optic lobes. During normal development, the R cells within each ommatidium innervate the optic lobe in a defined sequence. R8 projects through the incipient lamina and into the medulla. R1–R6 axons project along the surface of R8 and terminate between two rows of lamina glial cells. After a lag, the R7 cell projects through the lamina and into the developing medulla neuropil. R8 projections were assessed using mAb24B10 (prior to innervation by R7). R1–R6 topography and ganglion-specific targeting were assessed using an R4-specific marker, mδ−LacZ, and an R2–R5-specific marker, Rotau LacZ, and the R7 projections were assessed using

an R7-specific promoter PM181-Gal4 driving LacZ expression.

### *N-Cadherin Is Required for a Precise R8 Topographic Map in the Medulla*

R cell projections were visualized at the third larval stage with mAb24B10 (Figures 3A and 3B). In wild-type animals, R cell axons form a topographic map in which the spatial relationships between R cell axons correspond to the spatial relationships between ommatidia (Figure 3A). In eye-specific *N-cadherin* mosaic animals, topographic map formation was defective in both the lamina (see below) and the medulla (Figure 3B). As R1–R6 axons do not mistarget to the medulla (see below) and, at this stage of development, most R7 axons do not stain with mAb24B10, only the R8 growth cones are visualized in the medulla using mAb24B10. In wild-type, R8 axons form evenly spaced bundles in the medulla (Figure 3A). In *N-cadherin* mutants, this array was disrupted (Figure 3B). These aberrant R8 projections extended only a short distance away from their normal termination site. We infer that the topographic mapping defects are local and that the global topography of the pattern remains approximately normal.

### *N-Cadherin Is Required for Local Topographic Mapping in the Lamina but Not for Ganglion Specificity*

To assess whether the topographic mapping defect in *N-cadherin* mutants includes R1–R6 cells, we examined the organization of R1–R6 projections in the lamina of prepupae. Since mAb24B10 labels all mature R1–R6 axons, the resultant expression pattern in the lamina is too complex to resolve individual termini (Figure 3B). We therefore utilized a marker expressed only in a single R cell type, R4, to label only one fiber in each ommatidial axon bundle (Figures 3E–3H). In wild-type animals, R4 axons project into the lamina plexus, where their growth cones expand (Figures 3E and 3G). In *N-cadherin* mutants, the regular spacing of R4 growth cones was disrupted (Figures 3F and 3H). In addition, some R4 growth cones failed to expand in the lamina plexus.

While *N-cadherin* mutations disrupt local topographic mapping in the lamina, they do not affect ganglion specificity; R4 axons do not mistarget to the medulla. To confirm this observation, *N-cadherin* mutants were examined using the Ro-tau LacZ marker, which is expressed in R2, R3, R4, and R5. As in wild-type, these axons terminated in the lamina and did not extend into the medulla (Figures 3C and 3D).

### *R7 Axons Exhibit Abnormal Growth Cones, Defects in Topography, and Delayed Innervation of the Medulla Neuropil*

To assess the outgrowth of R7 growth cones into the optic lobe, we compared wild-type and *N-cadherin* mutant animals carrying an R7-specific axonal marker (Figures 3I and 3J). In wild-type animals initiating pupal development, R7 axons form a regular array of 10–12 rows of termini in the medulla. By contrast, in eye-specific mosaic *N-cadherin* flies, R7 projections are arranged in an irregular pattern, and the array of termini contains fewer rows (approximately six). In addition, in wild-type animals, the R7 growth cone undergoes a distinct morphological transition as it enters the medulla. Migrating R7 growth cones have a small "spear-like" morphology (data not shown), while R7 growth cones that have reached the target are expanded (Figure 3I). In mosaic *N-cadherin* flies, many R7 growth cones within the medulla exhibited an elongated and thickened morphology (Figure 3J). Although the guidance of R7 to its target was disrupted in *N-cadherin* mutants, the association between R7 and R8 axons from the same ommatidium was maintained (data not shown).

### *Lamina Neurons and Glial Cells Develop Normally when Innervated by* N-Cadherin *Mutant R Cells*

R cell axons induce the development of lamina neurons and glial cells. To exclude the possibility that the effects of *N-cadherin* mutations on R cell axon targeting result from effects on R cell-induced target differentiation, we examined development of the target region innervated by *N-cadherin* mutant R cells. Using the neuron-specific marker, Elav (Robinow and White, 1991), we observed that the columnar organization of the lamina neurons was normal in *N-cadherin* mosaic animals (data not shown). Expression of the glial cell-specific nuclear protein, Repo (Xiong et al., 1994), was normal in *N-cadherin* mutant mosaics, indicating that glial cells differentiated and migrated normally into the lamina (Figure 3L, compare to Figure 3K). However, the organization of glial cells was disrupted in *N-cadherin* mutant animals such that, in some localized regions of the lamina, they failed to form the three layers seen in wild-type.

In summary, N-cadherin is required for the local topographic mapping of R1–R6 in the lamina and R7 and R8 in the medulla. As R8 enters the target region first, and the remaining R cells then follow the R8 axon into the target, the defects seen for R1–R6 and R7 targeting may reflect earlier defects in R8 projections.

## *N-Cadherin* in R7 Growth Cones Regulates Target Specificity in the Medulla

A serious limitation in the studies described in the previous sections is that, while the target is wild-type in these mosaics, all R cell afferents are mutant. Deducing the specific mechanistic basis for any of the defects observed is made difficult by the large number of R cells that are missing *N-cadherin* and the known and possible interactions among these and other cells of the visual system. To gain a more precise appreciation of N-cadherin's role in R cell growth cones, it would be ideal to remove its function from a single R cell and to assess the consequences in animals in which the surrounding R cell axons and the target region are wild-type. Using various molecular and classical genetic manipulations, we have developed an approach to studying the effects of mutations in R7 cell axons surrounded by normal neighboring R cell axons and a normal target. In this section, we demonstrate that the selective loss of *N-cadherin* from R7 disrupts R7 target layer specificity and an R7-specific visual behavior.

### *Loss of N-Cadherin from R7 Neurons Alone Causes Their Inappropriate Termination in the R8 Target Layer of the Medulla*

To create and label homozygous mutant R7 cells, we used a strategy that exploits the fact that specific R cell types are generated by temporally separated mitoses. R2–R5 and R8 are derived from mitotic divisions that occur early in eye development (i.e., anterior to the morphogenetic furrow). The final cell division giving rise to

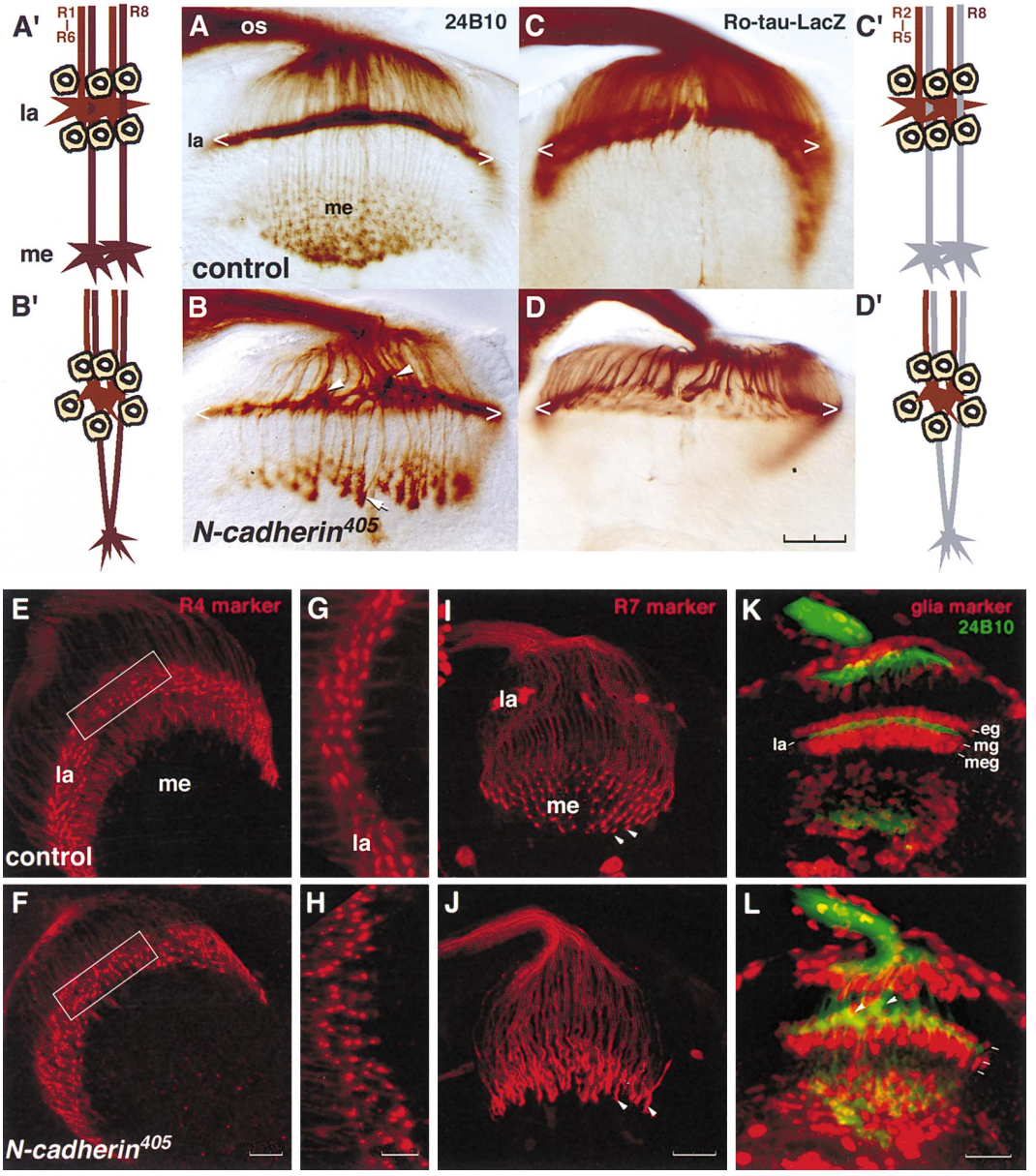


Figure 3. N-Cadherin Controls R Cell Local Topographic Mapping

(A, A′, C, C′, E, G, I, and K) Wild-type. (B, B′, D, D′, F, H, J, and L) *N-cadherin* eye-specific mosaic. Optic lobes were stained at the third larval stage (A–D and K–L) or prepupae (E–J).

(A and B) Optic lobe stained with the R cell-specific mAb24B10. os, optic stalk; la, lamina; me, medulla. Chevrons denote the position of the lamina plexus. In these preparations, the lamina plexus forms a smooth line of uniform thickness due to the expansion of R1–R6 growth cones, while R8 termini form a regular array in the medulla. In *N-cadherin* mosaic animals, the lamina plexus forms irregular clumps (arrowheads), while R8 termini exhibit defects in local topographic mapping (small arrow).

(A′ and B′) Schematic summaries of (A) and (B), respectively. R1–R6 axons are colored light brown; R8 is dark brown. The glial cells flanking the lamina plexus are yellow.

(C and D) LacZ is expressed in R2–R5 under the control of the Rough promoter (Ro-tau-LacZ). Chevrons denote the lamina plexus. In both wild-type and *N-cadherin* mosaic animals, all R2–R5 axons target correctly to the lamina.

(C′ and D′) Schematic summaries of (C) and (D). R2–R5 axons are colored brown; R8 is gray (unstained).

(E, F, G, and H) LacZ expression under the control of an R4-specific promoter. The regular array of R4 termini seen in wild-type is disrupted in *N-cadherin* mosaic animals.

(E and F) Low-magnification views, looking down onto the surface of the lamina. Boxes demarcate the regions depicted in (G) and (H).

(G and H) High-magnification views. The morphology of R4 growth cones is affected by the loss of N-cadherin activity as they do not expand fully within the lamina plexus.

8(I and J) LacZ expression under the control of an R7-specific promoter. In wild-type, the regular array of R7 termini is visible in the medulla. In *N-cadherin* mosaic animals, this array is irregular and the morphology of R7 termini is disrupted. R7s exhibit elongated thickening along the terminal region.

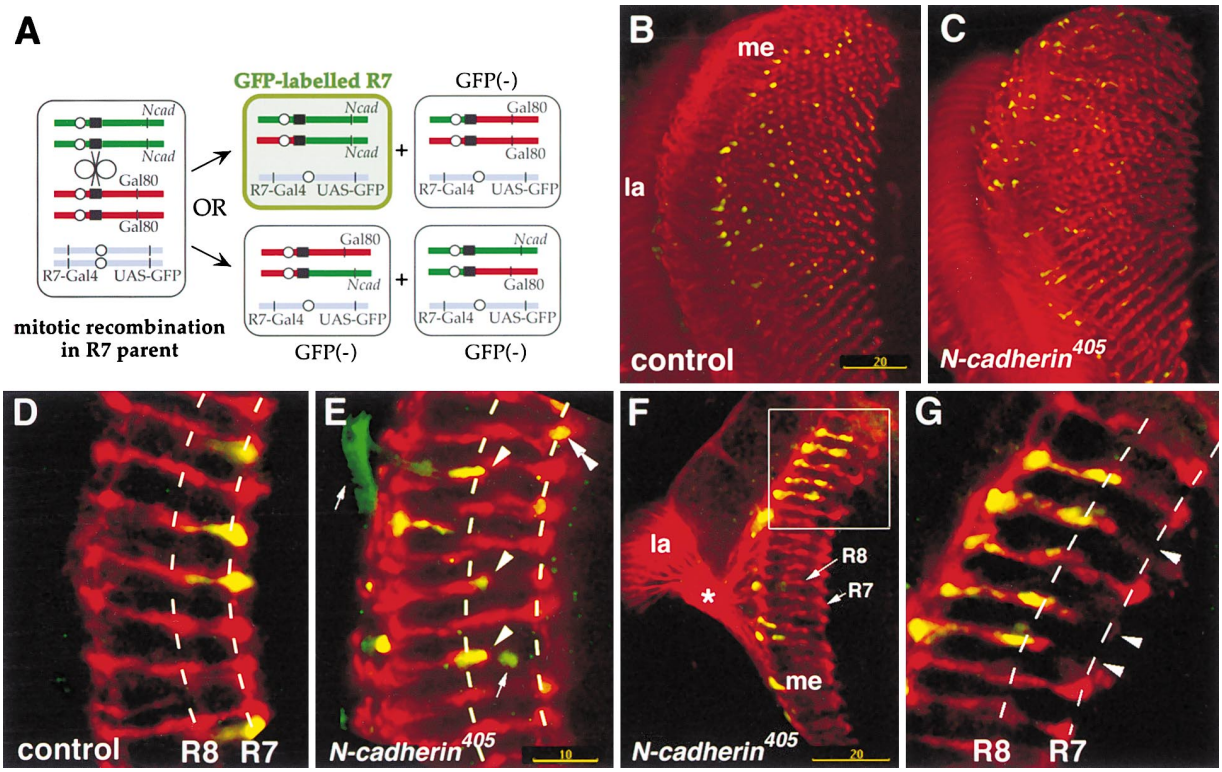


Figure 4. Single *N-Cadherin* Mutant R7 Axons Mistarget to the R8 Layer

(A) Schematic summary of selective labeling of single *N-cadherin* mutant R7 axons in adult flies using GMR-FLP and the MARCM system (see text). These axons are visualized using antibodies against GFP (green). As GFP is fused to the synaptic protein, synaptobrevin, the axon terminal but not the shaft is preferentially labeled. The axons of R7 and R8 were visualized using mAb24B10 (red).

(B and D) Wild-type.

(C and E–G) *N-cadherin* mutant.

(B and C) Low-magnification images displaying R7 and R8 termini in the medulla. The layer separation between R7 and R8 cannot been seen in this view. GFP-positive R7 axons were randomly distributed within the medulla, indicating that mitotic recombination occurred stochastically, in both control and *N-cadherin* mutant mosaic animals. In these *N-cadherin* mosaics, the overall topographic map is normal.

(D) High-magnification view. R7 cells homozygous for a wild-type FRT40A chromosome terminate at their appropriate layer, M6.

(E–G) *N-cadherin* mutant R7 axons fail to terminate at the R7 target layer, M6, and stop instead at the R8 layer, M3. Thus, N-cadherin is required specifically in R7 cells for them to properly target to the R7 target layer. Expression of GFP is observed in R7 axons whose termini are out of the plane of focus; this staining is not denoted. In (E), the arrowheads denote the terminals of mutant R7 axons that terminate in the R8 layer; double arrowheads denote a mutant R7 axon that has terminated correctly and arrows mark background tracheal staining. In (F), box indicates region displayed in (G). In (G), the arrowheads indicate regions of the R7 recipient that are not innervated by R cells because the corresponding R7 axons have innervated the R8 recipient layer instead. In (D), (E), and (G), dashed lines denote the R7 and R8 recipient layers. la, lamina; me, medulla neuropil; *, optic chiasm.

Scale bars: 20 μm in (B), (C), (F); 10 μm in (D), (E), (G).

R1, R6, and R7 cells occurs later in development (i.e., posterior to the morphogenetic furrow). We used the GMR enhancer to express FLP recombinase to drive mitotic recombination posterior to the furrow (Pignoni et al., 1997) (Figure 4A). This results in approximately 15% of R1s, R6s, and R7s being homozygous for a particular chromosomal arm (data not shown). To label exclusively the R7s that are homozygous for an *N-cadherin* mutation, we used the MARCM method (Lee and Luo, 1999) (Figure 4A). Briefly, a ubiquitously expressed Gal80 construct is present on the FRT chromosome homologous to that of the chromosome bearing the *N-cadherin* mutation. In addition, a UAS-synaptobrevin-GFP reporter construct activated by an R7-specific Gal4 is also present in the strain. The Gal80 construct dominantly represses Gal4-dependent transcription. Therefore, only cells that are homozygous for the *N-cadherin* chromosome will have lost the Gal80 repressor and, hence, will express GFP.

As predicted, we observed that approximately 15% of R7s were labeled with synaptobrevin-GFP (Figures

(K and L) Double labeling of optic lobes using the R cell specific marker mAb24B10 (green) and the glia-specific nuclear marker Repo (red).

(K) In wild-type, lamina glia form three layers: eg, equatorial glia; mg, marginal glia; meg, medulla glia. Each glia row is marked by a dash. la, lamina plexus.

(L) In *N-cadherin* mosaics, the lamina plexus is irregular (arrowheads) and lamina glia differentiate normally, although they form irregular rows.

Scale bars: 20 μm in (A)–(F) and (I)–(L); 10 μm in (G) and (H).

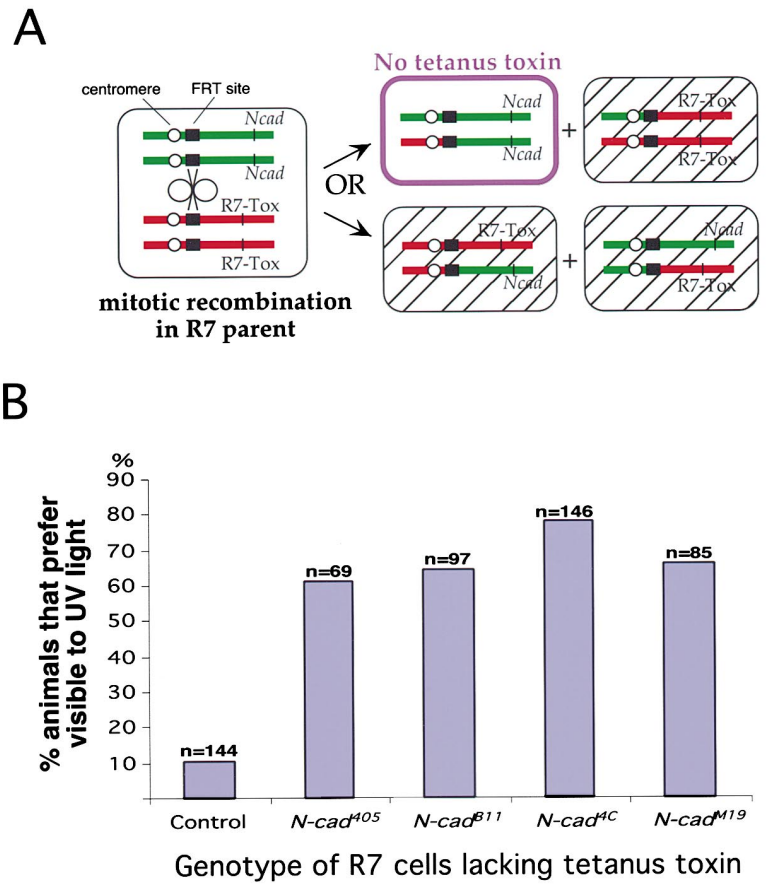


Figure 5. *N-Cadherin* Is Required in R7 Cells to Drive Normal Visual Behavior

(A) Targeted mitotic recombination generates flies dependent upon homozygous mutant R7 cells to drive the UV/Vis choice test (see text).

(B) *N-cadherin* is required for normal UV/Vis choice behavior. Flies (between 10 and 30) were tested for their ability to select UV over visible light. Each trial was on the order of 15 s. As variable numbers of flies were tested and the variation between trials was small, we have plotted the percentage of flies choosing UV light as a fraction of the total (n) tested for each genotype. R7-tox indicates tetanus toxin driven by an R7-specific promoter.

4B and 4C). When these R7s were homozygous for a wild-type chromosome, they terminated uniformly at the normal R7 target layer, M6 (Figure 4D). By contrast, when these R7s were homozygous for an *N-cadherin* mutation, most terminated incorrectly in the R8 target layer, M3 (Figures 4E–4G). We have assessed layer-specific targeting in all four *N-cadherin* alleles; each displayed quantitatively similar expressivity. Approximately 70% (n = 573) of mutant R7 axons mistargeted to the R8 recipient layer. However, local topographic mapping of R7 in the medulla appeared normal in these mosaic animals. In addition to terminating in the incorrect layer, the distribution of GFP-synaptobrevin in *N-cadherin* mutant R7 cells was also abnormal. In wild-type, synaptobrevin-GFP is largely localized to the extreme terminus of R7 in the M6 layer, presumably reflecting the targeting of synaptobrevin to R7 synapses. In contrast, in *N-cadherin* mutant R7s, synaptobrevin-GFP was seen not only at their termini but also along their lengths. This may indicate the failure of R7s to elaborate normal synapses with targets in the M3 layer, resulting in abnormal intracellular targeting of synaptobrevin-GFP. These data argue strongly that N-cadherin is required in R7 cells to promote their extension from the M3 to the deeper M6 layer.

### N-Cadherin *Mutant R7 Neurons Are Functionally Abnormal*

To test whether mistargeting of *N-cadherin* mutant R7 cells disrupts R7-dependent behaviors, we devised a method to assess behavior in flies in which N-cadherin was selectively removed from R7 cells (Figure 5A). R7s homozygous for *N-cadherin* mutations were generated using GMR-FLP (Figure 5A). A transgene, PANR7-Tox, which expresses tetanus toxin light chain in R7 cells, is present on the FRT chromosome homologous to that of the chromosome bearing the *N-cadherin* mutation. R7 cells that contain PANR7-Tox should be incapable of evoked synaptic transmission. Indeed, nonmosaic animals heterozygous for the PANR7-Tox construct phototaxed toward visible light in preference to UV, consistent with R7 function having been reduced or eliminated (data not shown). Therefore, in genetically mosaic animals generated using GMR-FLP, only the 15% of R7 cells that are homozygous for the *N-cadherin* mutant chromosome will have lost the PANR7-Tox and, hence, will be capable of evoked synaptic transmission.

In control experiments when some 15% of the R7 cells were homozygous for a wild-type chromosome, the resulting mosaic animals behaved normally in the UV/Vis choice test (Figure 5B). We then tested the behavior of animals in which these R7s were rendered homozygous for four different *N-cadherin* alleles. In each case, animals preferred visible to UV light suggesting that *N-cadherin* mutant R7s do not function normally (Figure 5B). Hence, the failure of *N-cadherin* mutant R7 neurons to reach their target layer in the medulla correlates with a behavioral deficit.

### N-Cadherin Is Expressed on R Cell Axons and within the Target Region

The distribution of N-cadherin protein was assessed at multiple stages during late larval and pupal development

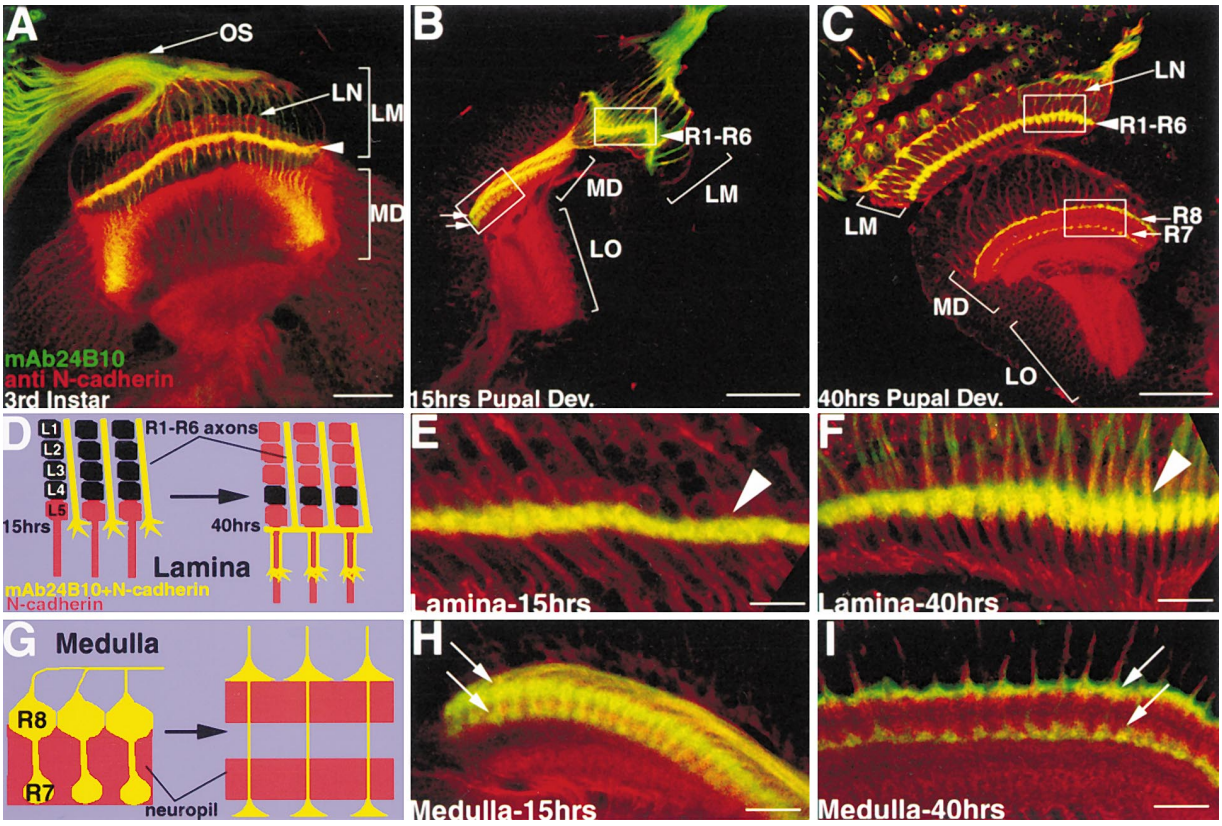


Figure 6. N-Cadherin Is Expressed on Both R Cells and in the Target Region

The distribution of N-cadherin was assessed at the third larval stage and at two stages during pupal development (15 hr and 40 hr). Each optic lobe was double-labeled using the R cell-specific mAb24B10 (green) and a polyclonal antibody against the N-cadherin intracellular domain (red). LM, lamina; MD, medulla; LO, lobula; OS, optic stalk; LN, lamina neurons; arrowhead, lamina plexus.

(A) Expression of N-cadherin at the third larval stage. In this view, the eye disc is to the left, and the optic lobe is viewed in cross section. N-cadherin is expressed on R cell axons, the lamina neuron L5, and tangential fibers within the medulla. N-cadherin expression is also observed in subretinal glia (faintly stained within the optic stalk).

(B, E, and H) Expression of N-cadherin at 15 hr of pupal development. (B) Low-magnification view of the optic lobe, presenting cross-sectional views of the lamina, medulla, and lobula. White boxes demarcate the regions displayed in (E) and (H). (E) High-magnification view of the lamina. N-cadherin is expressed in the lamina plexus and lamina neuron L5. At this stage of development, R1–R6 growth cones have not yet begun synaptic partner choice and remain within the plexus. (H) High-magnification view of the medulla. R7 and R8 termini have formed two layers (arrows). N-cadherin is expressed in both R7 and R8, as well as in the medulla neuropil between the two layers.

(C, F, and I) Expression of N-cadherin at 40 hr of pupal development. (C) Low-magnification cross-sectional view of the lamina, medulla, and lobula. White boxes demarcate the regions presented in (F) and (I). At this stage, R1–R6 growth cones have migrated out of the ommatidial bundle toward their synaptic partners. White arrows denote the R7 and R8 layers. N-cadherin is expressed in many lamina neurons and their axons at this stage, but not in glia. Strong N-cadherin staining is also seen in the developing medulla and lobula neuropils. (F) High-magnification view of the lamina. R cell axons have begun to extend down their target cartridge, thickening the lamina plexus. (I) High-magnification view of the medulla. The R7 and R8 layers are separated by two stripes of N-cadherin expression within the medulla neuropil.

(D and G) Schematic outline of the lamina (D) and medulla (G) during the transition from 15 hr to 40 hr of pupal development. R cell axons that express both N-cadherin and mAb24B10 are indicated in yellow; lamina neurons that express N-cadherin are indicated in red; lamina neurons that are unstained are denoted in black. In (G), the red stripes denote expression of N-cadherin within the medulla neuropil.

Scale bars: 50 μm in (B) and (C); 10 μm in (E), (F), (H), and (I).

using antibodies specific to either its extracellular or intracellular domain (Iwai et al., 1997) (Figure 6). Similar results were obtained with both antibodies. N-cadherin was expressed on all R cells as they differentiate and can be observed on the R8 axon as soon as it extends into the optic lobe (Figure 6A). Strong expression was visible within the lamina plexus, where R1–R6 axons terminate, and within the medulla, including the region containing R7 and R8 termini (Figure 6A). The expression pattern at the third larval stage is thus consistent with N-cadherin acting within R cell axons to control local topographic map formation in both the lamina and the medulla. N-cadherin immunoreactivity was observed also in the medulla neuropil, the developing lamina neuron L5 and the subretinal glial cells (Figure 6A). As we have not assessed the effects of removing N-cadherin specifically from these cells, N-cadherin may also function within them to contribute to patterns of R cell connectivity.

N-cadherin remains expressed on R1–R6 cell axons as they select lamina targets during midpupal development (Figures 6C, 6D, 6F, 6G, and 6I). We also observed strong expression within several lamina target neurons in each column at this stage (data not shown). Conversely, we

were unable to detect significant N-cadherin staining on any lamina glial cells, although the possibility that N-cadherin might be expressed on these cells at a low level cannot be excluded. These observations are consistent with a direct role for N-cadherin during target selection within the lamina.

To assess the expression of N-cadherin at the developmental stage when the layer-specific targeting of R7 is taking place, we followed N-cadherin expression during the early phases of pupal development (Figures 6B, 6D, 6E, 6G, and 6H). At this stage of development, there is a gradient of developmental stages distributed across the medial/lateral axis of the medulla (i.e., from left to right in Figure 6H) with the youngest R cell axons arriving at the lateral edge. The R7 and R8 terminals lie in two distinct layers in early pupal development with strong mAb24B10 and N-cadherin colocalization observed in the presumptive R8 layer and with weaker staining within the future R7 layer (Figures 6G and 6H). As R7 axons arrive later than R8s, there is a clear gradient of innervation within the R7 layer. In addition to expression in R7 and R8, N-cadherin was expressed in the region of the medulla neuropil between them but was not expressed at high levels in the region immediately above R8 or below R7.

To confirm that the R8 and R7 terminals are indeed separate at this early stage, we examined expression of an R7-specific axonal marker, PM181-Gal4, driving a membrane-tethered GFP reporter (UAS-mCD8-GFP). Expression of this marker in R7 commences prior to axonogenesis and, hence, can be used to label R7 growth cones early in their development. In contrast, mAb24B10 recognizes an antigen expressed in the R7 cell approximately 12 hr later. Using this R7-specific marker, we observed that the R7 growth cone arrives in the medulla and immediately extends past the R8 layer (Figures 7A and 7B). Moreover, as R8 but not R7 expresses mAb24B10 at this early stage, we also confirmed that the R8 axon does not extend into the R7 target layer.

## Discussion

Using behavioral screens, we identified multiple alleles of *N-cadherin* that affect R cell connectivity. Defects in local topographic mapping of R cell axons were observed both in the lamina and medulla. In the lamina, R1–R6 neurons did not project to their specific lamina targets, although they did remain within their appropriate layer. N-cadherin is expressed in many regions of the developing optic ganglia consistent with a role in establishing connections of many different classes of neurons. To gain a more precise assessment of the role of N-cadherin function in connection formation, we selectively removed it from R7 neurons in an otherwise largely wild-type background. R7 neurons that lacked N-cadherin selectively terminated in the R8 layer, M3, rather than extending to the R7 layer, M6. These data provide strong genetic evidence that N-cadherin regulates the formation of precise patterns of neuronal connections.

### N-Cadherin Plays a Pleiotropic Role in R Cell Connectivity

Members of the cadherin family have been implicated in multiple aspects of axon guidance and targeting. For example, antibody perturbation experiments demonstrate that N-cadherin is required for the proper termination of retinal ganglion cell axons in the chick tectum (Inoue and Sanes, 1997). In addition, using dominant-negative constructs, frog N-cadherin was shown to regulate axonogenesis in retinal ganglion cells (Riehl et al., 1996). N-cadherin also mediates multiple functions in the fly (Iwai et al., 1997). In the embryonic CNS, N-cadherin plays a role in axon fasciculation and causes specific neuronal subsets to adopt abnormal trajectories. These functions of N-cadherin could be attributed to its known homophilic or its potential heterophilic binding properties. As the extracellular domains of *Drosophila* N-cadherin contains more cadherin repeats, as well as additional domains not found in vertebrate N-cadherins (Iwai et al., 1997), it remains unclear whether they are functionally equivalent.

We have uncovered multiple guidance functions of N-cadherin in different neuronal cell types of the visual system. In R8 cells, N-cadherin is required for the formation of the normal topographic map. These defects likely reflect a role for N-cadherin in mediating interactions between R8 axons. N-cadherin is also essential for R1–R6 axons to choose correct synaptic partners in the lamina. In *N-cadherin* mutants, R1–R6 axons do not defasciculate from the ommatidial bundle and fail to reach their targets. This defect likely reflects a loss of N-cadherin-mediated interactions between R cell axons or between R cell growth cones and lamina neurons. N-cadherin is also required for R7 target specificity (discussed below). The observed pleiotropy in N-cadherin's cellular functions is seen for many guidance molecules and highlights the importance of analyzing mutant phenotypes at the level of single mutant cells in an otherwise wild-type background.

### N-Cadherin Acts in R7 to Control Target Specificity

By analyzing individual *N-cadherin* mutant R7s in a mostly wild-type background, we uncovered a function of N-cadherin in target specificity. In particular, individual *N-cadherin* mutant R7 axons failed to terminate in the R7 target layer, M6, and instead terminated in the R8 target layer, M3. One simple model (Figure 7C) to explain the role of N-cadherin in R7 target selection is that it mediates homophilic adhesion between R7 growth cones and processes in the medulla neuropil. This adhesive interaction may promote R7 axon extension into the M6 layer. Indeed, the expression pattern of N-cadherin within the medulla neuropil is consistent with this view: N-cadherin is expressed throughout the region of R7 axon extension. Alternatively, N-cadherin could stabilize contact between the R7 terminus and processes in its target layer. Consistent with this notion, N-cadherin expression is observed later in pupal development in both the R7 terminals and surrounding medulla neuropil.

Our analysis suggests that, just as there is a choice point at which R cell axons decide whether to terminate

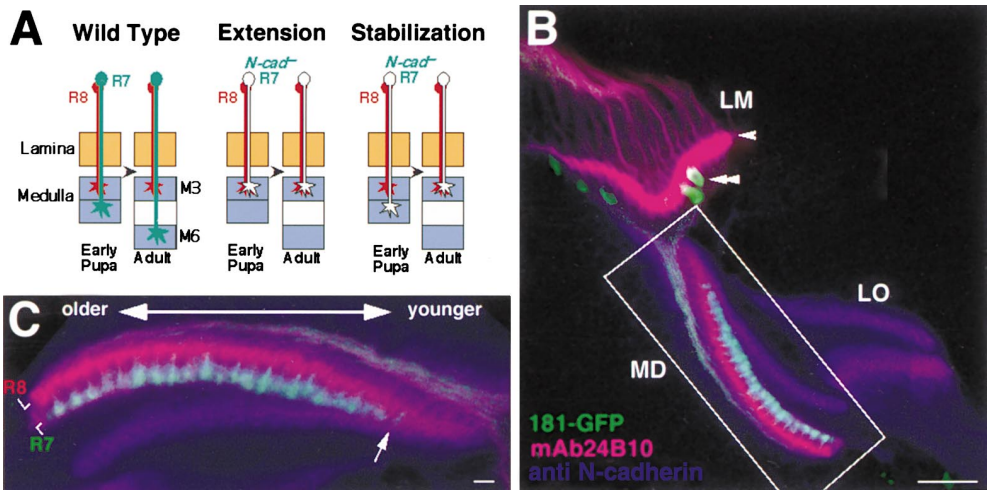


Figure 7. N-Cadherin Is Required for R7 Target Specificity

(A) A schematic view of R7 target selection in wild-type and two possible models for how selective loss of N-cadherin from R7 results in the adult phenotype observed. In wild-type, the R7 growth cone extends past the layer containing R8 growth cones as soon as it arrives in the medulla (B and C). In the extension model, N-cadherin-mediated adhesion is required for the initial extension of R7 into the correct target layer. In the stabilization model, *N-cadherin* mutant R7 cells make this extension correctly but require N-cadherin-mediated adhesion to stabilize the initial contact with the R7 target layer.

(B and C) In wild-type, the separation between R7 and R8 growth cones in the medulla was assessed at 15 hr after puparium formation. R7 axons expressed PM181-Gal4, UAS-mCD8-GFP and were visualized with antibodies against GFP (green); R8 axons were visualized with mAb24B10 (pink) and N-cadherin protein (blue). LM, lamina; MD, medulla; LO, lobula; arrowhead, lamina plexus; double arrowhead, a GFP-positive lamina cell. The boxed region in (B), comprising the medulla, is shown at higher magnification in (C).

(C) The medulla is viewed in cross section such that newly innervating R7 growth cones (arrow) are to the right and older R7 growth cones are to the left. The layer of R8 growth cones and the layer of R7 growth cones are indicated. R7 expression of PM181-Gal4, UAS-mCB8-GFP marker precedes R7 axonogenesis. In younger R7 growth cones, mAb24B10 is not detected. It is detected in older R7 growth cones. mAb24B10 staining is specific to R8 in younger regions of the medulla. These data indicate that R7 and R8 terminals are separated early in medulla development. Scale bars: 20 μm in (B); 4 μm in (C).

in the lamina or continue through to the medulla, there is a choice point for R7 and R8 axons in the medulla. Here R8 axons remain in the presumptive M3 layer while R7 axons extend further and terminate within presumptive M6. R7 layer selection occurs immediately upon entry of R7 terminals into the medulla region. Remarkably, at this early stage the termination sites differ by only 2–3 μm in distance. Further experiments examining mutant R7 growth cones as they extend into a normal target will resolve whether N-cadherin is required in R7 for the initial selection of the appropriate layer or stabilization of the R7-target interaction (Figure 7C).

As N-cadherin is expressed by both R7 and R8, differential expression of N-cadherin cannot account for the different choices made by these two growth cones. We envision that additional regulatory mechanisms account for the differences in R7 and R8 target selection. Interestingly, mutations in a receptor tyrosine phosphatase, PTP69D, exhibit R7 targeting defects similar to those observed in *N-cadherin* mutants, although it is not known whether PTP69D functions in R7 cells or other R cell axons (Newsome et al., 2000). Regulation of N-cadherin activity by receptor tyrosine phosphatases has been reported: the vertebrate receptor tyrosine phosphatase μ (PTPμ) can physically associate with N-cadherin and modulate its activity (Brady-Kalnay et al., 1995, 1998). In particular, disrupting PTPμ function in vitro slows outgrowth of retinal ganglion axons on an N-cadherin substrate (Burden-Gulley and Brady-Kalnay, 1999). This result suggests that PTPμ can positively regulate N-cadherin-mediated interactions that are required for axon outgrowth. It will be interesting to assess in future experiments whether differential regulation of N-cadherin activity by receptor tyrosine phosphatases at the R7/R8 choice point accounts for the differences in target selection made by these two axons.

## Cadherins Have Been Proposed to Control Synaptic Specificity

Synapse formation is thought to require two types of interactions (reviewed in Shapiro and Colman, 1999). First, interactions mediated by specific adhesion molecules match synaptic partners. And second, less specific adhesion molecules "lock in" these transient associations. The remarkable diversity of the known cadherin family members expressed in neurons, particularly of the CNR class, has led to the view that cadherins might define part of the "synaptic code" that mediates the initial recognition of synaptic partners (Kohmura et al., 1998; Wu and Maniatis, 1999). That is, specificity of the homophilic and heterophilic interactions possible for each cadherin might direct the interactions between neurons expressing different cadherins or combinations of them, leading to the formation of specific connectivity patterns (Serafini, 1999). In addition, functional studies, as well as immunolocalization experiments, are consistent with the idea that cadherins also regulate synapse stability (Fannon and Colman, 1996; Uchida et al., 1996; Benson and Tanaka, 1998). In particular, experiments using antibodies and peptides to block N- and E-cadh-

erin function demonstrated that these molecules are required for the changes in synaptic efficacy that underlie long-term potentiation in the hippocampus (Tanaka et al., 2000; Tang et al., 1998).

Our results on the requirement for N-cadherin activity in R7 to mediate target layer choice are interesting to consider in the context of models for cadherin function in synaptic specificity in vertebrates. N-cadherin may be required for R7 to recognize processes within the R7 recipient layer. This may represent the initial contact involved in the formation of specific synaptic connections. As we have not explored the relationship between layer selection and the formation of specific synapses, this view remains speculative. Nevertheless, the similarity to the models proposed for vertebrate cadherins is striking.

## R7 Synaptic Connection Formation as a Model for Target Specificity

Previous studies have demonstrated that the R7 neuron is an excellent system for studying pattern formation at the level of individual identifiable cells (reviewed in Zipursky and Rubin, 1994; Dickson, 1995). As we demonstrate in this paper, R7 is also an attractive model for studying mechanisms regulating the formation of specific neuronal connections. Using a combination of classical and molecular genetic techniques, we can manipulate R7 neurons selectively. This enables us to assess the role of genes in R7 independent of their roles in other R cell afferents or in the target. Indeed, as we demonstrated in this paper, while genes such as N-cadherin may play pleiotropic roles in the development of connections in the visual system, selective removal of N-cadherin from R7 revealed a precise function at a discrete choice point.

While the ability to selectively manipulate the genetics of R7 provides an insightful analytical methodology, it also provides a powerful genetic screen for mutations disrupting R7 connectivity. Using targeted mitotic recombination, we can generate eyes in which the only functional R7 cells are homozygous for randomly mutagenized chromosomes. This small fraction of R7 cells (about 15%) is sufficient to drive wild-type behavior in the UV/Vis light phototactic choice test. Indeed, this fraction is close to a functional threshold and hence the screen provides a sensitive means of identifying mutants. We anticipate that genetic screens for mutations disrupting R7 connectivity will lead to important insights into the mechanisms controlling targeting and synapse formation as well as a better understanding of the roles of N-cadherin and other interacting components in this process.

## Experimental Procedures

### Genetics

Fly stocks were maintained at 22°C on standard medium and mutagenized using ethylmethane sulfonate following standard procedures (Ashburner, 1989; Grigliatti, 1986). Details of the screens will be published elsewhere. Briefly, eye-specific mosaic flies were generated using the FLP/FRT method in which FLP expression is controlled by an eyeless promoter fragment and a cell lethal mutation (*cycE*$^{AR95}$) is used to reduce the size of the twinspot (Newsome et al., 2000). Mosaic flies without visible morphological defects in the retina were screened for the optomotor and UV/Vis response. FRT40A mosaic flies were used as controls.

To generate *N-cadherin* mutant R7 cells, we used GMR-FLP to induce mitotic recombination in the precursors that give rise to R1, R6, and R7 cells. To specifically label *N-cadherin* mutant R7 cells, we used the MARCM method (Lee and Luo, 1999). To reduce background GFP expression in wild-type R7 axons, mosaic animals were grown at 18°C. *N-cadherin* mutant R7 cells were also generated in a background in which the synaptic activity of nonmutant R7s was suppressed. We engineered a tetanus toxin light chain fragment (Sweeney et al., 1995) under the control of the PANR7 promoter (P. Beaufils and C. Desplan, personal communication) onto an FRT chromosome homologous to that of *N-cadherin* and used GMR-FLP to induce mitotic recombination.

### Histology

R cell projections were examined using mAb24B10 staining in combination with either HRP/DAB visualization or fluorescent 2° antibody staining followed by confocal laser scanning microscopy (Bio-Rad MRC 1024) (Martin et al., 1995; Garrity et al., 1999). The following markers specific to different R cell subtypes were used. Ro-tau-LacZ was used for R2-R5 projections (Garrity et al., 1999) and mδ-LacZ for R4 (Cooper and Bray, 1999). PM181-Gal4 (the PM181 promoter was a gift from E. Hafen) was combined with a reporter, UAS-LacZ, and used to examine R7 projections in the third larval stage. Another R7-specific driver, PANR7-Gal4 (P. Beaufils and C. Desplan, personal communication), was combined with a reporter, UAS-Synaptobrevin-GFP (Estes et al., 2000), and used to examine R7 projections in adult flies. This reporter system is expressed strongly in R7 cells, but we have also observed a low level of expression in the R8 cells of *sevenless* flies. This background expression in R8 was never observed when the marker is used as part of the GMR-FLP/MARCM system. The following concentrations of primary antibodies were used: mAb24B10, 1:200 dilution; mouse anti-LacZ antibody (Promega), 1:200 dilution; rat anti-Repo antibody, 1:100 dilution; rabbit anti-GFP (Clontech), 1:200 dilution; and rat anti-N-cadherin (against the intracellular domain of N-cadherin, a gift from T. Uemura), 1:20 dilution. The secondary antibodies goat anti-rabbit or mouse IgG coupled to FITC, Cy3, or Cy5 (Jackson Immunoresearch) were used in a 1:200 dilution. For cryostat sections of adult fly brains, see Garrity et al. (1996). For DiI injection, see Clandinin and Zipursky (2000). For silver staining of paraffin sections, see Gregory (1980) and Heisenberg and Bohl (1979).

### Behavioral Assays

The optomotor response was assayed in clear plastic tubes (2.5 cm diameter, 27 cm long) using groups of approximately 50 flies, 3–7 days old, with age-matched controls. Response was elicited using a moving bar of white light approximately 0.75 cm wide, moving at 1.5 m/s at an overall illumination of approximately 7 lux. Each trial was 1 min long; each group of flies was tested twice in succession. The UV/Vis test was performed as described (Reinke and Zipursky, 1988), using light intensities that were optimized for the isogenic control stock. Each trial was approximately 15 s long. Each group contained 10–30 flies and was tested three times. The counter current phototaxis assay was performed as described (Benzer, 1967), using clear plastic tubes and groups of approximately 30 flies. Each group was tested several times. Roughly equal numbers of males and females were tested in each trial for each behavior.

### Western Blots

Stage 16 embryos were homogenized in SDS sample buffer. After brief centrifugation, samples were electrophoresed on an SDS-PAGE gel and were immunoblotted with antibody to the C-terminal intracellular domain of N-cadherin.

### Acknowledgments

We thank members of the Zipursky lab for comments on the manuscript and Tadashi Uemura, Barry Dickson, Ernst Hafen, and Claude Desplan for reagents and communication of results prior to publication. We also thank Seymour Benzer for the optomotor apparatus prototype. This work was supported by a postdoctoral fellowship

from the Jane Coffin Childs Foundation (T.R.C.), the Burroughs-Wellcome Fund for Biomedical Research (T.R.C.), the Helen Hay Whitney Foundation (T.H.), the Life Sciences Research Foundation (HHMI) (C.-H.L.), and an MSTP NIH grant #GM08042 (R.L.). S.L.Z. is an investigator of the Howard Hughes Medical Institute.

Received December 21, 2000; revised February 21, 2001.

**References**

Ashburner, M. (1989). *Drosophila*: A Laboratory Manual (Cold Spring Harbor, NY: Cold Spring Harbor Laboratory Press).

Benson, D.L., and Tanaka, H. (1998). N-cadherin redistribution during synaptogenesis in hippocampal neurons. J. Neurosci. *18*, 6892–6904.

Benzer, S. (1967). Behavioral mutants of *Drosophila* isolated by countercurrent distribution. Proc. Natl. Acad. Sci. USA *58*, 1112–1119.

Brady-Kalnay, S.M., Rimm, D.L., and Tonks, N.K. (1995). Receptor protein tyrosine phosphatase PTPmu associates with cadherins and catenins in vivo. J. Cell Biol. *130*, 977–986.

Brady-Kalnay, S.M., Mourton, T., Nixon, J.P., Pietz, G.E., Kinch, M., Chen, H., Brackenbury, R., Rimm, D.L., Del Vecchio, R.L., and Tonks, N.K. (1998). Dynamic interaction of PTPmu with multiple cadherins in vivo. J. Cell Biol. *141*, 287–296.

Burden-Gulley, S.M., and Brady-Kalnay, S.M. (1999). PTPmu regulates N-cadherin-dependent neurite outgrowth. J. Cell Biol. *144*, 1323–1336.

Clandinin, T.R., and Zipursky, S.L. (2000). Afferent growth cone interactions control synaptic specificity in the *Drosophila* visual system. Neuron *28*, 427–436.

Cooper, M.T., and Bray, S.J. (1999). Frizzled regulation of Notch signaling polarizes cell fate in the *Drosophila* eye. Nature *397*, 526–530.

Detrick, R.J., Dickey, D., and Kintner, C.R. (1990). The effects of N-cadherin misexpression on morphogenesis in *Xenopus* embryos. Neuron *4*, 493–506.

Dickson, B. (1995). Nuclear factors in sevenless signalling. Trends Genet. *11*, 106–111.

Estes, P.S., Ho, G.L., Narayanan, R., and Ramaswami, M. (2000). Synaptic localization and restricted diffusion of a *Drosophila* neuronal synaptobrevin—green fluorescent protein chimera in vivo. J. Neurogenet. *13*, 233–255.

Fannon, A.M., and Colman, D.R. (1996). A model for central synaptic junctional complex formation based on the differential adhesive specificities of the cadherins. Neuron *17*, 423–434.

Fischbach, K.-F., and Dittrich, A.P.M. (1989). The optic lobe of *Drosophila* melangaster. I. A golgi analysis of wild-type structure. Cell Tissue Res. *258*, 441–475.

Flanagan, J.G., and Vanderhaeghen, P. (1998). The ephrins and Eph receptors in neural development. Annu. Rev. Neurosci. *21*, 309–345.

Fujita, S.C., Zipursky, S.L., Benzer, S., Ferrus, A., and Shotwell, S.L. (1982). Monoclonal antibodies against the *Drosophila* nervous system. Proc. Natl. Acad. Sci. USA *79*, 7929–7933.

Garrity, P.A., Rao, Y., Salecker, I., McGlade, J., Pawson, T., and Zipursky, S.L. (1996). *Drosophila* photoreceptor axon guidance and targeting requires the Dreadlocks SH2/SH3 adapter protein. Cell *85*, 639–650.

Garrity, P.A., Lee, C.-H., Salecker, I., Robertson, H.C., Desai, C.J., Zinn, K., and Zipursky, S.L. (1999). Retinal axon guidance in *Drosophila* is regulated by a receptor protein tyrosine phosphatase. Neuron *22*, 707–717.

Gerresheim, F. (1981). Isolation and characterization of mutants with altered phototactic reaction to monochromatic light in *Drosophila* melanogaster. PhD thesis, Munich University, Munich, Federal Republic of Germany.

Gregory, G.E. (1980). The Bodian Protargol technique. In Neuroanatomical Techniques, N.J. Strausfeld and T.A. Miller, eds. (New York; Springer-Verlag), pp. 75–95.

Grigliatti, T. (1986). Mutagenesis. In *Drosophila*: A Practical Approach, D.B. Roberts, ed. (Oxford, IRL press), pp. 39–48.

Harris, W.A., Stark, W.S., and Walker, J.A. (1976). Genetic dissection of the photoreceptor system in the compound eye of *Drosophila* melanogaster. J. Physiol. *256*, 415–439.

Heisenberg, M., and Bohl, K. (1979). Isolation of anatomical brain mutants of *Drosophila* by histological means. Z. Naturforsch. *34*, 143–147.

Heisenberg, M., and Buchner, E. (1977). The role of retinula cell types in the visual behavior of *Drosophila* melanogaster. J. Comp. Physiol. *117*, 127–162.

Inoue, A., and Sanes, J.R. (1997). Lamina-specific connectivity in the brain: regulation by N-cadherin, neurotrophins, and glycoconjugates. Science *276*, 1428–1431.

Iwai, Y., Usui, T., Hirano, S., Steward, R., Takeichi, M., and Uemura, T. (1997). Axon patterning requires DN-cadherin, a novel neuronal adhesion receptor, in the *Drosophila* embryonic CNS. Neuron *19*, 77–89.

Kohmura, N., Senzaki, K., Hamada, S., Kai, N., Yasuda, R., Watanabe, M., Ishii, H., Yasuda, M., Mishina, M., and Yagi, T. (1998). Diversity revealed by a novel family of cadherins expressed in neurons at a synaptic complex. Neuron *20*, 1137–1151.

Lee, T., and Luo, L. (1999). Mosaic analysis with a repressible neurotechnique cell marker for studies of gene function in neuronal morphogenesis. Neuron *22*, 451–461.

Martin, K.A., Poeck, B., Roth, H., Ebens, A.J., Conley Ballard, L., and Zipursky, S.L. (1995). Mutations disrupting neuronal connectivity in the *Drosophila* visual system. Neuron *14*, 229–240.

Meinertzhagen, I.A., and Hanson, T.E. (1993). The development of the optic lobe. In The Development of *Drosophila* melanogaster, M. Bates and A.M. Arias, eds. (cold Spring Harbor, New York: Cold Spring Harbor University Press), pp. 1363–1492.

Miskevich, F., Zhu, Y., Ranscht, B., and Sanes, J.R. (1998). Expression of multiple cadherins and catenins in the chick optic tectum. Mol. Cell. Neurosci. *12*, 240–255.

Miyatani, S., Shimamura, K., Hatta, M., Nagafuchi, A., Nose, A., Matsunaga, M., Hatta, K., and Takeichi, M. (1989). Neural cadherin: role in selective cell-cell adhesion. Science *245*, 631–635.

Newsome, T.P., Asling, B., and Dickson, B.J. (2000). Analysis of *Drosophila* photoreceptor axon guidance in eye-specific mosaics. Development *127*, 851–860.

Pignoni, F., Hu, B., Zavitz, K.H., Xiao, J., Garrity, P.A., and Zipursky, S.L. (1997). The eye-specification proteins So and Eya form a complex and regulate multiple steps in *Drosophila* eye development. Cell *91*, 881–891.

Reinke, R., and Zipursky, S.L. (1988). Cell-cell interaction in the *Drosophila* retina: the bride-of-sevenless gene is required in the photoreceptor cell R8 for R7 cell development. Cell *55*, 321–330.

Riehl, R., Johnson, K., Bradley, R., Grunwald, G.B., Cornel, E., Lilienbaum, A., and Holt, C.E. (1996). Cadherin function is required for axon outgrowth in retinal ganglion cells in vivo. Neuron *17*, 837–848.

Robinow, S., and White, K. (1991). Characterization and spatial distribution of the ELAV protein during *Drosophila* melanogaster development. J. Neurobiol. *22*, 443–461.

Serafini, T. (1999). Finding a partner in a crowd: neuronal diversity and synaptogenesis. Cell *98*, 133–136.

Shan, W.S., Tanaka, H., Phillips, G.R., Arndt, K., Yoshida, M., Colman, D.R., and Shapiro, L. (2000). Functional cis-heterodimers of N- and R-cadherins. J. Cell Biol. *148*, 579–590.

Shapiro, L., and Colman, D.R. (1999). The diversity of cadherins and implications for a synaptic adhesive code in the CNS. Neuron *23*, 427–430.

Stowers, R.S., and Schwarz, T.L. (1999). A genetic method for generating *Drosophila* eyes composed exclusively of mitotic clones of a single genotype. Genetics *152*, 1631–1639.

Suzuki, S.C., Inoue, T., Kimura, Y., Tanaka, T., and Takeichi, M. (1997). Neuronal circuits are subdivided by differential expression of type-II classic cadherins in postnatal mouse brains. Mol. Cell. Neurosci. *9*, 433–447.

Sweeney, S.T., Broadie, K., Keane, J., Niemann, H., and O'Kane, C.J. (1995). Targeted expression of tetanus toxin light chain in *Drosophila* specifically eliminates synaptic transmission and causes behavioral defects. Neuron *14*, 341–351.

Tanaka, H., Shan, W., Phillips, G.R., Arndt, K., Bozdagi, O., Shapiro, L., Huntley, G.W., Benson, D.L., and Colman, D.R. (2000). Molecular modification of N-cadherin in response to synaptic activity. Neuron *25*, 93–107.

Tang, L., Hung, C.P., and Schuman, E.M. (1998). A role for the cadherin family of cell adhesion molecules in hippocampal long-term potentiation. Neuron *20*, 1165–1175.

Tessier-Lavigne, M.T., and Goodman, C.S. (1996). The molecular biology of axon guidance. Science *274*, 1123–1133.

Uchida, N., Honjo, Y., Johnson, K.R., Wheelock, M.J., and Takeichi, M. (1996). The catenin/cadherin adhesion system is localized in synaptic junctions bordering transmitter release zones. J. Cell Biol. *135*, 767–779.

Wohrn, J.C., Nakagawa, S., Ast, M., Takeichi, M., and Redies, C. (1999). Combinatorial expression of cadherins in the tectum and the sorting of neurites in the tectofugal pathways of the chicken embryo. Neuroscience *90*, 985–1000.

Wu, Q., and Maniatis, T. (1999). A striking organization of a large family of human neural cadherin-like cell adhesion genes. Cell *97*, 779–790.

Xiong, W.C., Okano, H., Patel, N.H., Blendy, J.A., and Montell, C. (1994). repo encodes a glial-specific homeo domain protein required in the *Drosophila* nervous system. Genes Dev. *8*, 981–994.

Yagi, T., and Takeichi, M. (2000). Cadherin superfamily genes: functions, genomic organization, and neurologic diversity. Genes Dev. *14*, 1169–1180.

Yamagata, M., Herman, J.P., and Sanes, J.R. (1995). Lamina-specific expression of adhesion molecules in developing chick tectum. J. Neurosci. *15*, 4556–4571.

Zipursky, S.L., and Rubin, G.M. (1994). Determination of neuronal cell fate: lessons from the R7 neuron of *Drosophila*. Annu. Rev. Neurosci. *17*, 373–397.